



**HAL**  
open science

# Performance Assessment of a New Flat Sepiolite Clay-Based Ultrafiltration Membrane for the Removal of Paracetamol and Indigo Blue Dyes from Two Synthetic Aqueous Solutions

Mohamed Romdhani, Wala Aloulou, Hajer Aloulou, Joelle Duplay, Catherine Charcosset, Raja Ben Amar

## ► To cite this version:

Mohamed Romdhani, Wala Aloulou, Hajer Aloulou, Joelle Duplay, Catherine Charcosset, et al.. Performance Assessment of a New Flat Sepiolite Clay-Based Ultrafiltration Membrane for the Removal of Paracetamol and Indigo Blue Dyes from Two Synthetic Aqueous Solutions. *Sustainability*, 2024, 16 (5), pp.1860. 10.3390/su16051860 . hal-04720010

**HAL Id: hal-04720010**

**<https://hal.science/hal-04720010v1>**


Submitted on 18 Oct 2024

**HAL** is a multi-disciplinary open access archive for the deposit and dissemination of scientific research documents, whether they are published or not. The documents may come from teaching and research institutions in France or abroad, or from public or private research centers.

L'archive ouverte pluridisciplinaire **HAL**, est destinée au dépôt et à la diffusion de documents scientifiques de niveau recherche, publiés ou non, émanant des établissements d'enseignement et de recherche français ou étrangers, des laboratoires publics ou privés.

## Article

# Performance Assessment of a New Flat Sepiolite Clay-Based Ultrafiltration Membrane for the Removal of Paracetamol and Indigo Blue Dyes from Two Synthetic Aqueous Solutions

Mohamed Romdhani<sup>1,2</sup>, Wala Aloulou<sup>1</sup>, Hajer Aloulou<sup>1,3</sup>, Joelle Duplay<sup>4,\*</sup> , Catherine Charcosset<sup>2</sup> and Raja Ben Amar<sup>1,\*</sup>

<sup>1</sup> Research Unit “Advanced Technologies for Environment and Smart Cities”, Faculty of Science of Sfax, University of Sfax, Sfax 3038, Tunisia; med594268@gmail.com (M.R.); walaaloulou6@gmail.com (W.A.); hajer.aloulou89@yahoo.fr (H.A.)

<sup>2</sup> LAGEP, UMR 5007, CNRS, Université Claude Bernard Lyon 1, 43 Boulevard du 11 Novembre 1918, F-69100 Villeurbanne, France; catherine.charcosset@univ-lyon1.fr

<sup>3</sup> Department of Chemistry, Preparatory Institute for Engineering Studies of Gabes, Gabes 6029, Tunisia

<sup>4</sup> ITES, UMR 7063, CNRS, Université de Strasbourg, F-67084 Strasbourg, France

\* Correspondence: jduplay@unistra.fr (J.D.); benamar.raja@yahoo.com (R.B.A.)

**Abstract:** In the last decade, the development of a new generation of membranes based on low-cost materials has been widely studied. These membranes demonstrate significantly higher performance than the conventional ceramic membranes currently used in membrane separation technology. This work is focused on the development of a low-cost flat UF ceramic membrane composed completely of sepiolite using a uniaxial pressing method with dimensions of 5.5 cm of diameter and 3 mm of thickness. The sintering temperatures used were from 650 to 800 °C. Several properties, such as morphology, porosity, permeability, mechanical strength, and chemical resistance, are investigated. The results show that the mean pore diameter is increased from 40 to 150 nm when the sintering temperature increases from 650 °C to 800 °C. At these temperatures, excellent mechanical strength of 18 MPa to 22 MPa and high chemical resistance were achieved. SEM results revealed a crack-free structure with a uniformly smooth surface. Permeability tests were conducted using dead-end filtration. The sepiolite membrane demonstrated an improvement in its water permeability from 18 to 41 L·m<sup>-2</sup>·h<sup>-1</sup>·bar<sup>-1</sup> when the sintering temperature increased from 650 °C to 750 °C. The efficiency of the sepiolite membranes sintered at 650 °C and 700 °C were evaluated with the application of the removal of paracetamol (PCT) and indigo blue (IB) dye separately from two synthetic aqueous solutions representing the pharmaceutical and textile sectors. Excellent removal efficiency of almost 100% for both contaminants was observed at ambient temperature and a pressure of 3 bars. Membrane regeneration was achieved through simple rinsing with deionized water. According to this finding, the UF sepiolite membrane demonstrated reversible fouling, which is consistent with the fouling coefficient “FRR” value higher than 90%.

**Keywords:** sepiolite; ceramic membrane; removal; paracetamol; indigo blue dye



**Citation:** Romdhani, M.; Aloulou, W.; Aloulou, H.; Duplay, J.; Charcosset, C.; Ben Amar, R. Performance Assessment of a New Flat Sepiolite Clay-Based Ultrafiltration Membrane for the Removal of Paracetamol and Indigo Blue Dyes from Two Synthetic Aqueous Solutions. *Sustainability* **2024**, *16*, 1860. <https://doi.org/10.3390/su16051860>

Academic Editor: Md. Shahinoor Islam

Received: 8 January 2024

Revised: 17 February 2024

Accepted: 21 February 2024

Published: 23 February 2024



**Copyright:** © 2024 by the authors. Licensee MDPI, Basel, Switzerland. This article is an open access article distributed under the terms and conditions of the Creative Commons Attribution (CC BY) license (<https://creativecommons.org/licenses/by/4.0/>).

## 1. Introduction

Over the last few years, the consumption of drinking water representing a very limited part of the total available water resources has continued to rise, principally due to industrial expansion, especially in various developing nations of the world. Consequently, water quality decreased irreversibly due to the increase in the load of numerous pollutants in the environment.

The industrial sectors are considered to be the highest water consumers after the agricultural sector [1]. Textile and pharmaceutical industries are very water-intensive [2,3] and consequently produce large quantities of contaminated wastewater due to the use

of dyes and various chemical agents [4,5], resulting in environmental degradation when untreated wastewater is discharged.

The production of dyes per year was estimated as 800,000 tons, including 200,000 tons of textile dyes [6]. In addition, different types of pharmaceutical compounds, including analgesics, anti-inflammatory drugs, and antibiotics, are released into the environment following their use. These substances have been detected in water resources. Moreover, improper or unlawful disposal of pharmaceutical waste can significantly contribute to environmental pollution [7]. Many findings confirm that dyes and pharmaceutical compounds can have serious damage to the environment and human health [8,9]. According to Mittal [10], artificial dyes can cause several adverse effects like cancer, allergies, and hyperactivity in children. Furthermore, the presence of high levels of pharmaceutical compounds in wastewater poses a risk to human health and impacts the ecosystem.

Regarding human health, it has been reported that serious harmful effects, such as gene toxicity, disruption of the endocrine system, and cancer could be caused by these contaminants [11]. Consequently, it is of vital importance to have access to efficient water treatment technology for resolving this problematic.

According to the literature [12,13], several technologies have been applied for treating wastewater, including coagulation–flocculation, adsorption, photocatalysis, ion exchange, and membrane separation processes. Membrane processes have emerged as promising substitutes for wastewater treatment and reuse in several industrial applications [14,15] and have exhibited many interesting benefits compared to other technologies [16], such as operational simplicity, ease of process automation, low space requirement and long-life performance [14,17].

Nowadays, membrane separation processes, such as ultrafiltration (UF), nanofiltration (NF), and reverse osmosis (RO), are widely used for the removal of organic and inorganic contaminants from wastewater [18].

In general, NF is the most effective process for removing dyes and pharmaceuticals [19,20]. However, due to its small pore size, high pressure is required, which increases the operating cost [21,22]. Ultrafiltration represents a cheaper process; however, by operating with conventional UF membranes, dye and pharmaceutical substances could not be eliminated effectively due to the larger membrane pore diameter in comparison to the size of these substances.

Ceramic membranes are characterized by better retention properties, higher permeability, and less susceptibility to fouling [23,24]. According to the literature, the use of ceramic membranes has gained attention in various industrial applications compared to polymeric membranes [18] due to their good chemical and thermal stability, high mechanical strength, and longer life [18,25].

Generally, commercialized ceramic membranes are mostly fabricated from metallic oxides, such as alumina ( $\text{Al}_2\text{O}_3$ ), zirconia ( $\text{ZrO}_2$ ), glass ( $\text{SiO}_2$ ), and titania ( $\text{TiO}_2$ ). These materials are chosen for their interesting properties, such as excellent mechanical, thermal, and chemical stability, ensuring prolonged durability. However, the use of these materials leads to a high cost of manufactured ceramic membrane due to the high sintering temperature usually needed (between 1400 °C and 1600 °C) and the high cost of the membrane starting materials [18].

Therefore, considerable attention has been paid by researchers to reduce the cost of ceramic membrane preparation while maintaining high performance. Several researchers have focused on the development of low-cost ceramic membrane manufacturing based on cheap raw materials, such as natural clay, apatite powder, dolomite, kaolin, zeolite, smectite, bentonite, sepiolite, and mineral coal fly ash [14,26,27].

In this context, flat bentonite membranes have been successfully developed for textile wastewater treatment [28,29]. Bouazizi et al. [28] prepared flat sheet ceramic membranes based on natural bentonite mixed with low amount of starch as porosity agent. It was found that this membrane, sintered at 950 °C, exhibited high performance in terms of mechanical and chemical stabilities with uniform porosity. Saja et al. [25] used natural

perlite to elaborate a microfiltration membrane with a sintering temperature of 950 °C. This membrane performed well when applied to the treatment of food and tannery effluents. Reporting to the finding of Bousbih et al. [30], a UF membrane made from a mixture of natural kaolin clay, Amijel (as plasticizer), Methocel (as binder), and starch (as porosity agent), sintered at 1000 °C, was prepared. This UF membrane exhibits good performance in the treatment of two textile effluents.

Despite the various studies on the fabrication of low-cost ceramic membranes based on low-cost materials, such as clay, some constraints, such as the need for the addition of organic additives like plasticizer, binder, and a porosity agent are crucial from an environmental point of view because their disadvantages of causing air pollution during the process of sintering are already mentioned in the literature [18]. In this context, the fabrication of exclusively clay membrane is poorly described in the literature. Moreover, the study of the possibility of a decrease in the temperature during the sintering phase can be considered another interesting aspect as it has a determining effect on energy consumption during membrane fabrication and on membrane cost.

Natural sepiolite is a mineral hydrous magnesium silicate clay that can be considered a suitable material in ceramic membrane manufacturing due to its low-cost, low-sintering temperature and abundance in nature [31,32]. This low-cost material is a typical nanofibrous clay with a structural formula of  $\text{Si}_{12}\text{O}_{30}\text{Mg}_8(\text{OH})_4(\text{H}_2\text{O})_4 \cdot 8\text{H}_2\text{O}$  [33]. In their pristine form, sepiolite fibers exhibit microporosity with noteworthy rheological and adsorption characteristics. Each sepiolite fiber reveals a distinctive arrangement of silicate blocks and interconnected tunnels, extending in the same direction of the fiber. These blocks comprise an octahedral magnesium oxide/hydroxide sheet wedged between tetrahedral silicate sheets. The terminal magnesium ions found at the octahedral sheet edges form bonds with coordinated water molecules [34]. Furthermore, silanol (Si-OH) groups are positioned along the blocks' external edges, creating opportunities for activation of sepiolite properties [33].

To the best of our knowledge, few studies have investigated the use of sepiolite as a starting material for ceramic membrane preparation. One example is the use of sepiolite for ceramic UF membrane preparation using dispersing method [31].

The current study reports the elaboration and characterization of flat UF ceramic membrane exclusively made from natural sepiolite clay without any additional additives or porosity agent which represents the novelty of this study. The potential of the novel UF membrane to remove indigo blue dye (IB) and paracetamol (PCT) from synthetic aqueous solutions was evaluated.

## 2. Experimental

### 2.1. Raw Material

Raw sepiolite material from Turkey was ground for further processing in a planetary ball mill (Retsch PM 100). This procedure was performed using six stainless steel balls at a rotation speed of 300 rpm for 5 min. The resulting material was sieved through a sieve of 100 µm. This milling process ensured adequate mixing and milling of the sepiolite particles, resulting in homogenized and purified material ready for subsequent experiments and membrane development.

### 2.2. Flat Membrane Preparation

Flat sepiolite membranes were prepared using the uniaxial pressing technique, as described in Figure 1. The sepiolite powder (<100 µm) was homogeneously mixed with a few drops of water and then uniformly dispersed in a stainless steel mold to press under a pressure of 100 KN for 6 min. By applying such high pressure, the sepiolite particles are compacted and tightly packed to form a dense and uniform disk. The membranes were then sintered in a programmed oven at various temperatures with a plateau at 300 °C for 2 h to remove impurities. The final heating temperature according to the program of

temperature increase was between 650 °C and 800 °C. A low heating rate of 2 °C/min was chosen to avoid cracking formation in the ceramic membrane.

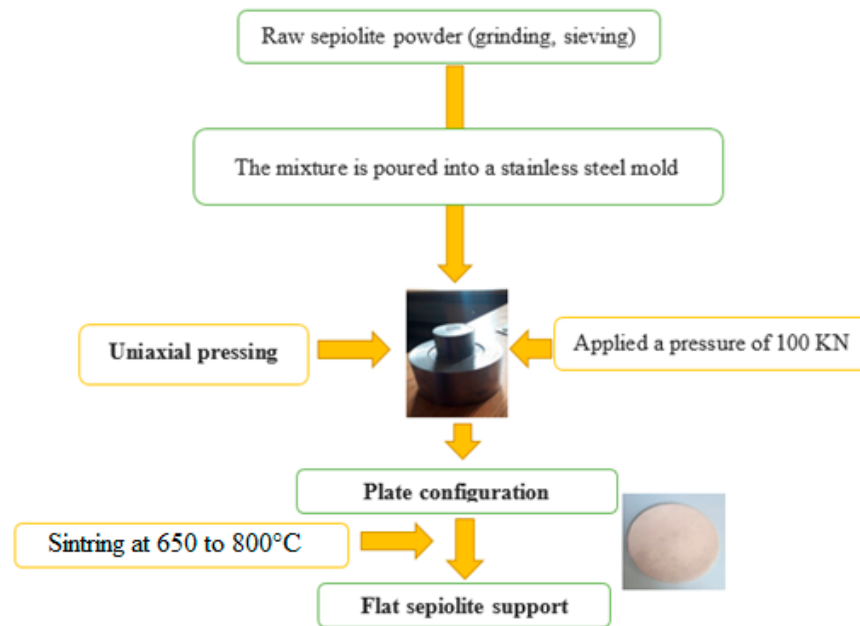


**Figure 1.** Scheme of preparation of flat ceramic membrane using the pressing method.

### 2.3. Characterization

X-ray diffraction (XRD) of the sepiolite sample was performed using a powder diffractometer (Bruker D8 Advance diffractometer was manufactured by Bruker Corporation, with headquarters in Billerica, MA, USA.) with CuK radiation ( $\lambda = 1.5418 \text{ \AA}$ ) scanning from  $4^\circ$  to  $60^\circ$  in  $2\theta$  scans. The chemical composition of the raw sepiolite was determined through atomic absorption (Perkin-Elmer was manufactured by PerkinElmer, Waltham, MA, USA). Simultaneous thermogravimetric (TGA) and differential scanning calorimetry (DSC) analyses were performed with an SDT Q600 V20.9 build 20 (TA Instruments, New Castle, DE, USA) thermal gravimetric analyzer (between 22 and 900 °C) at a heating rate of 10 °C/min under nitrogen atmosphere. A Zeiss MERLIN scanning electron microscope (SEM, Carl Zeiss, Merlin, Germany) was used for the examination of the membrane morphology. The determination of the particle size distribution (PSD) of the sepiolite was performed using a Mastersizer 2000 instrument (Malvern Instruments, Malvern, Worcestershire, UK). The mechanical resistance was measured according to the three-point bending test using a Lloyd mechanical testing machine (model LRX, Lloyd Instruments, Fareham, UK). The porosity was determined by using the principle of Archimedes [35]. This method is based on the following steps: The sepiolite membrane was first weighed dry to obtain its dry mass ( $M_d$ ). Then, the submerged mass ( $M_{sub}$ ) of the membrane immersed in distilled water was weighted. Finally, the membrane was taken out of the distilled water, and the excess liquid on the the membrane surface was wiped off with tissue paper to weight the saturated mass ( $M_{sat}$ ). The sepiolite membrane porosity  $P$  (%) was calculated using the following Equation (1):

$$P(\%) = \frac{M_{sat} - M_d}{M_{sat} - M_{sub}} \quad (1)$$

The chemical resistance of the support was assessed by weight loss after soaking in a concentrated solution of HCl with a pH of 1.5 and NaOH solution with a pH of 13 for 3 days.

Finally, to evaluate the removal efficiency of PCT and IB through sepiolite membranes, a UV-Vis spectrophotometer (UV 7205 JENWAY spectrophotometer, London, UK) was used. Contaminant concentrations were measured at specific wavelengths using 245 nm for paracetamol and 620 nm for indigo blue dye. The turbidity was measured using a

turbidimeter (HACH, model 2100A, Ames, IA, USA) before and after the experiment. A pH meter (SevenCompact pH meter S220, Mettler Toledo, Greifensee, Switzerland) was used to measure the pH during the experiment. These instruments enabled accurate and precise analysis of concentration levels and pH values, allowing us to assess the effectiveness of the membranes in removing paracetamol and indigo blue dye contaminants.

#### 2.4. Filtration Experiments

Filtration tests were performed using a laboratory dead-end filtration system, as shown in Figure 2. The flat membrane, with a filtration area of  $19.6210^{-4} \text{ m}^2$ , was initially immersed for 24 h in distilled water before being placed in the membrane module. Membrane filtration was performed in a pressured system using compressed air at room temperature.

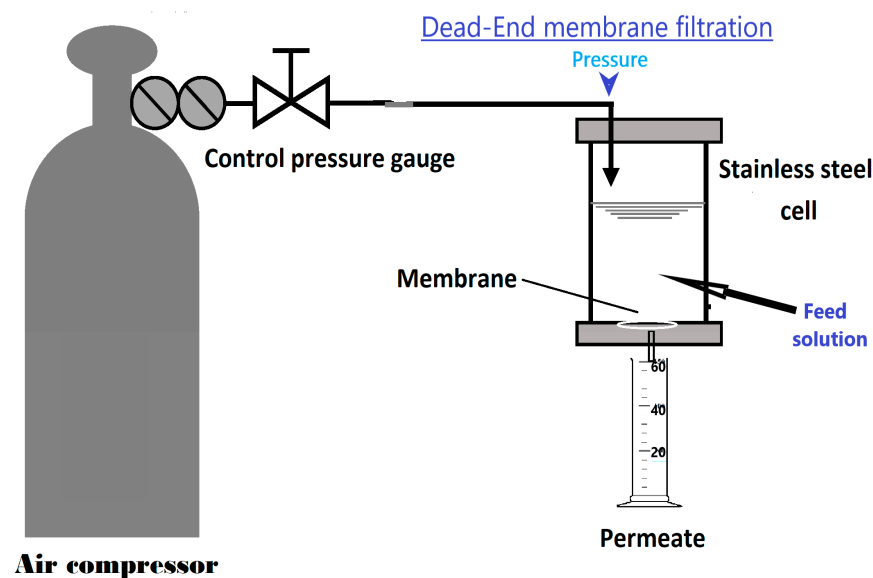


**Figure 2.** Schematic representation of laboratory dead-end filtration system.

The permeate flux ( $J_w$ ) was determined by measuring the time required to collect a fixed volume of permeate, as described in Equation (2):

$$J_w = \frac{V}{t \cdot A} \quad (2)$$

where  $V$  is the volume of permeate,  $t$  is the time, and  $A$  is the surface area of the membrane.

Permeability values ( $L_p$ ) were determined, according to Darcy's law [36], by calculating the slope of a linear plot of distilled water flux and applied transmembrane pressure ( $\Delta P$ ), according the following Equation (3):

$$J_w = L_p \cdot \Delta P \quad (3)$$

To evaluate the retention efficiency of the elaborated sepiolite membrane, IB dye and PCT aqueous solutions were used as synthetic effluents.

The IB dye and PCT were provided, respectively, by SITEX company located in Ksar Hellal (Tunisia) [36] and Dar Essaydaly pharmaceutical company located in Sfax (Tunisia).

The concentration of the permeate was measured using UV spectrophotometry and compared with the initial concentration to determine the retention percentage, as given by Equation (4):

$$R(\%) = \left(1 - \frac{C_p}{C_o}\right) \cdot 100 \quad (4)$$

where  $R(\%)$  represents the retention of the contaminant,  $C_o$  and  $C_p$  refer, respectively, to the initial concentration and the permeate concentration in mg/L.

### 2.5. Evaluation of the Fouling Resistance Capacities

The evaluation of the fouling resistance abilities in the sepiolite membrane system was conducted during filtration at a pressure of 3 bar for both synthetic contaminated solutions. Two coefficients, the flux recovery ratio (FRR) and the flux decay ratio (FDR) [37], were determined using the following equations:

$$\text{FDR} = \left( J_w - \frac{J_c}{J_w} \right) \cdot 100 \quad (5)$$

$$\text{FRR} = \left( \frac{J_{wa}}{J_w} \right) \cdot 100 \quad (6)$$

where  $J_w$  refers to the water permeate flux of the clean membrane,  $J_c$  denotes the stabilized permeate flux of the membrane when treating contaminated water, and  $J_{wa}$  refers to the water permeate flux of the membrane measured after rinsing with distilled water following water treatment. A higher FDR value indicates a greater decrease in the permeate flux, showing a higher susceptibility to fouling, while a higher FRR value indicates better recovery of the permeate flux after cleaning, demonstrating the membrane's ability to regain its initial performance. FDR and FRR may be calculated and compared to determine the UF membrane's capacity to resist fouling [38].

## 3. Results and Discussion

### 3.1. Characterization of Sepiolite Powder

#### 3.1.1. Chemical Analysis

The chemical composition of raw sepiolite, as mentioned in Table 1, indicates that the main constituents are silica and magnesium oxides with percentages of 51.2% and 27.68%, respectively, in addition to the presence of a minor amount of other components, such as calcium, potassium, and iron oxide.

**Table 1.** Chemical composition of raw sepiolite.

Parameters	LOI *	SiO <sub>2</sub>	MgO	CaO	Fe <sub>2</sub> O <sub>3</sub>	Na <sub>2</sub> O	K <sub>2</sub> O
Sepiolite (phase %)	14.3	51.2	27.68	5.49	0.12	0.15	0.03

\* Loss of ignition.

#### 3.1.2. Granulometry by Laser Diffraction of Sepiolite

The laser granulometry test of sepiolite particles, obtained after grinding and sieving through a sieve of 100  $\mu\text{m}$ , provides information about the size distribution and relative abundance of different particle sizes. As shown in Figure 3, the majority of the sepiolite particles (>89%) were smaller than 100  $\mu\text{m}$ . The presence of a small percentage greater than or equal to 100  $\mu\text{m}$  can be explained by the shape and the irregularities of the sepiolite particles. Also, sepiolite particles may tend to form clusters or agglomerates due to their physical and surface properties, leading to the presence of some particles larger than 100  $\mu\text{m}$ . In addition, the sepiolite particles exhibited a wide range of particle sizes. The majority (73%) of sepiolite particles have diameters within the range of 2–63  $\mu\text{m}$ . This suggests that the sepiolite sample consists of a significant proportion of particles in the fine to medium size range.

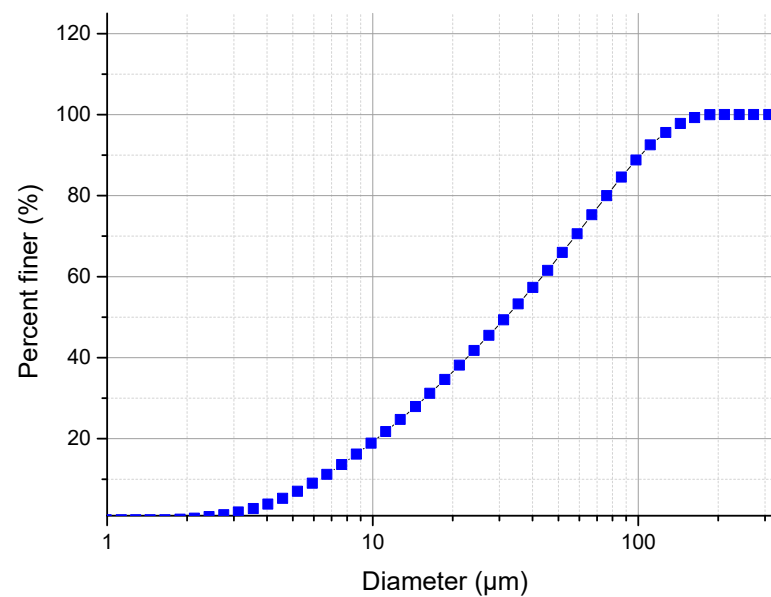


**Figure 3.** Particle size distribution of natural sepiolite.

### 3.1.3. X-ray Diffraction

XRD analysis is a fast analytical technique mainly used to obtain information about the crystalline components present in raw sepiolite. As shown in Figure 4, the strong and intense peak was centered at  $2\theta$  of  $7.2^\circ$ , which is comparable to the JCPDS card (70-1597) for the sepiolites [39]. This peak presents the main sepiolite characteristic reflection of the layer spacing  $d_{110} = 12 \text{ \AA}$  [39,40]. Other characteristic reflections of sepiolite occurring at  $2\theta$  of  $11.7^\circ$ ,  $17.7^\circ$ ,  $19.7^\circ$ ,  $20.6^\circ$ ,  $28.2^\circ$ ,  $34.9^\circ$ , and  $39.6^\circ$  were present. Notably,  $2\theta$  of  $20.7^\circ$  corresponds to quartz characteristics, while  $2\theta$  of  $29.5^\circ$  is attributed to carbonate impurities. Based on the aforementioned results, XRD analysis showed the same structural characteristics as the previous literature [39,40].

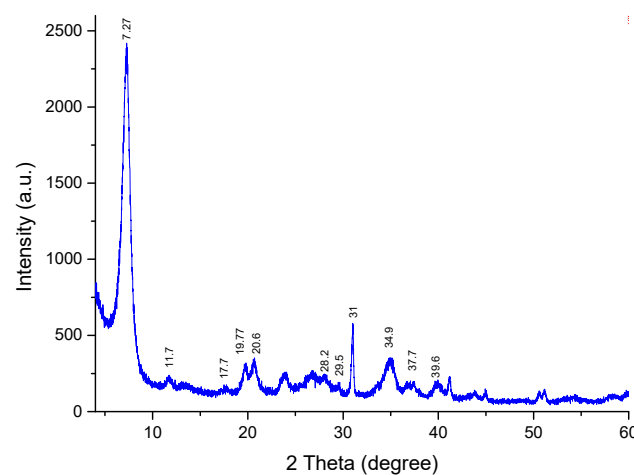


**Figure 4.** XRD spectrum of natural sepiolite used in this study.

### 3.1.4. Thermal Analysis

TGA and DSC analyses were performed using a single instrument to characterize the thermal properties and behavior of the material. Figure 5 shows the coupled TGA and DSC analyses of the raw sepiolite. The weight changes of the sample when the temperature increased show that about 11% of weight loss occurred between  $22^\circ\text{C}$  and  $130^\circ\text{C}$  due to evaporation or loss of water in the sample. The temperature of weight loss corresponds to the water boiling point at a standard atmospheric pressure of about  $100^\circ\text{C}$ . Consequently,



the weight loss of 11% indicates that the sample contains a significant amount of water, which is associated with the endothermic peak at 68 °C [33]. A mass loss of 5.8% in the temperature range of 150 °C and 461 °C, combined with an endothermic peak at 281 °C, corresponds with the release of the bound water from the sepiolite [33,41]. The mass losses of 6.7% and 2.13% associated with the decomposition of the carbonate impurities and the dehydroxylation process occurred in the temperature ranges 500–685 °C and 690–900 °C, respectively. Also, the thermal treatment in the range of 500–685 °C can be attributed to the dehydration of the strongly bound water from sepiolite clay. In a previous study, the temperature range of 730–860 °C indicated the loss of structural water, which lead to little change in the sepiolite structure [42]. The exothermic peak at 850 °C indicates the transformation of sepiolite into orthoenstatite ( $\text{MgSiO}_3$ ) [33,41]. This phenomenon was the result of bound water losses, which were in coordination with terminal  $\text{Mg}^{2+}$ ; consequently, the terminal  $\text{Mg}^{2+}$  in the octahedral layer was coordinated with the silica layer. In a similar vein, Zhang et al. [43] focused on phase transformation and morphological evolution by investigating the effects of thermal treatment on sepiolite fibers. They observed that significant crystal transformations occurred in the sepiolite at temperatures above 810 °C, which indicates that the thermal treatment allows a change in the crystal structure of the sepiolite.

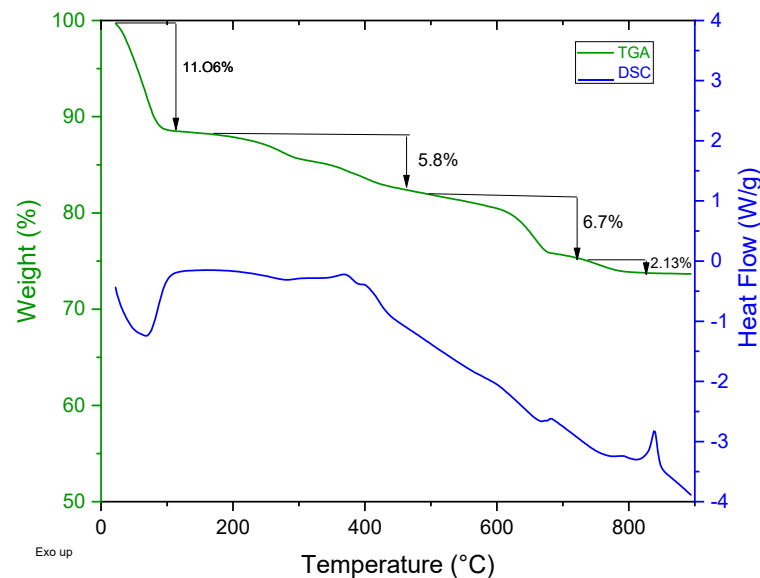


**Figure 5.** Thermal analysis curve of natural sepiolite used in this study.

### 3.2. Characterization of the Sepiolite Membranes

#### 3.2.1. Visual Inspection

The flat sepiolite membranes were produced using the uniaxial pressing method and sintered at different temperatures from 650 to 800 °C. At first, the color of the sepiolite membranes was white during the sintering process at different temperatures. This indicates that the thermal treatment has not caused significant changes in the membrane color. The uniform white color demonstrates that the composition and surface properties of the sepiolite membrane are relatively stable under the conditions of tested sintering. In addition, the configuration of the flat membranes was maintained even after being exposed to different temperatures ranging from 650 to 750 °C. It is important to highlight that the membrane surfaces are homogenous without any significant deformation or macrodefects in this temperature range. However, the sepiolite membrane surface, treated at 800 °C, showed significant deformation, making it not suited for the filtration process. This indicates that the treatment process above 800 °C exceeds the threshold at which the sepiolite membrane can maintain its structural integrity.

These visual inspection results provide valuable information about the behavior of sepiolite membranes in the sintering process. The uniform white color of the sepiolite membranes indicates that the composition remains stable and that no significant chemical reactions or impurities affect the color. However, at a temperature of 800 °C, the structure of the membrane is compromised.

### 3.2.2. Determination of Water Permeability

Water permeability,  $L_P$  (L/h·m<sup>2</sup>·bar), is an important factor in determining the optimal operating conditions for the membrane. To evaluate permeability, a test was conducted using distilled water at a pressure range of 1–4 bar. As shown in Figure 6, the evolution of the water permeability with pressure follows Darcy's law, and the water permeabilities for the S650, S700, and S750 membranes were 18, 39, and 41 L/h·m<sup>2</sup>·bar, respectively. This behavior was consistent with previous studies, as reported in the literature [44,45]. The increase in permeability  $L_P$  with increasing sintering temperatures is likely attributable to the corresponding enlargement of the pore sizes, strengthening the influence of pore size on membrane permeability characteristics [45].

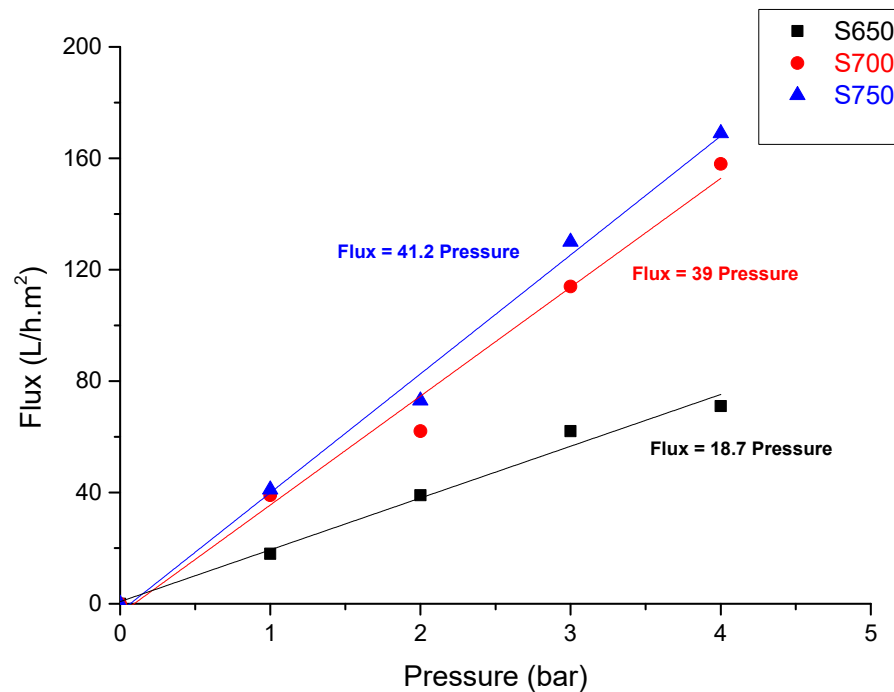


**Figure 6.** Permeability of S650 and S700 membranes.

### 3.2.3. Mechanical Strength and Porosity

Mechanical resistance tests were conducted using three-point bend strength to evaluate the effect of the sintering temperature (from 650 °C to 750 °C) on sepiolite membrane resistance. All the treated membranes at temperatures ranging from 650 °C to 750 °C exhibit excellent mechanical strength. The mechanical strength increased from 18 MPa to 22 MPa as the sintering temperature increased. This behavior was observed and confirmed by the literature results that the mechanical strength is strongly affected by the variation of the sintering temperature [28,46]. Increased mechanical strength with increasing sintering temperature indicates that higher temperatures promote stronger intermolecular bonds and improve the overall structural integrity and densification phenomena of the sepiolite membrane [25,46].

Contrary to the mechanical strength, as shown in Figure 7, the porosity decreased with an increasing in sintering temperature. This result is consistent with the trends found in the literature [38,44], indicating that an increase in the sintering temperature promotes particle fusion and compaction, thereby reducing the overall porosity of the sepiolite membrane.

This densification leads to a decrease in the volume of void spaces within the material, resulting in a more compact and homogeneous structure which reduces the porosity.

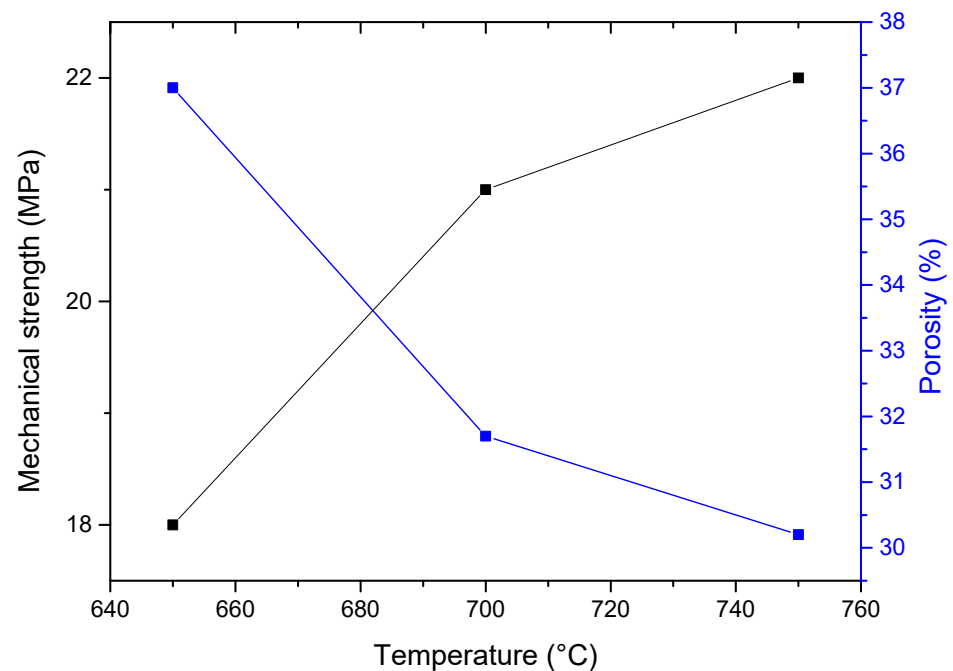


**Figure 7.** Variation of mechanical strength and porosity with sintering temperature.

#### 3.2.4. Chemical Resistance

Chemical resistance is an important parameter to evaluate the membrane material because the use of a filtration system requires that the membranes are regularly cleaned and regenerated. Therefore, various cleaning solutions such as enzymes, acids, and bases are usually used, especially acids and bases [14]. Therefore, the chemical resistance of sepiolite membrane was studied, as illustrated in Table 2. It is clear that the sepiolite membranes treated at 650 °C and 700 °C (S650 and S700) exhibit a good chemical resistance in acidic and basic media with a loss of weight less than 3%. However, better chemical resistance was observed in acidic media. The weight loss after 3 days of immersion did not exceed 1.3 wt.%. The presence of silicate minerals in the composition of sepiolite and their fibrous structures are responsible for their resistance to both media [33,47]. The prolonged exposure (3 days) can explain the slight loss of weight due to certain ions deteriorating or leaching. The membrane treated at 750 °C (S750) presented relatively poor chemical resistance, with a weight loss of up to 6% in both media. Based on the results of the thermal analysis, this behavior can be attributed mainly to thermal transformations and structural changes occurring during high-temperature treatments like decomposition and dehydroxylation processes and, consequently, more active functional groups [33,41].

**Table 2.** The effect of the sintering temperature on the mechanical strength, chemical resistance, permeability, and porosity of sepiolite membranes.

Membranes	Mechanical Strength (MPa)	Chemical Resistance (after 3 Days)		$L_p$ (L/h·m <sup>2</sup> ·bar)	Porosity (%)
		% Weight Lost in Acidic Medium	% Weight Lost in Basic Medium		
S650	18	1.01	2.69	18	37
S700	21	1.26	2.73	39	31.7
S750	22	6.61	7.2	41	30.2

Therefore, S650 and S700 membranes are retained for subsequent studies conducted on the application of UF for the removal of PCT and IB dye from contaminated solution.

### 3.2.5. SEM Characterization

The SEM results for the S650 and S700 membranes at different magnifications (600  $\mu\text{m}$ , 2  $\mu\text{m}$  and 200 nm) provide useful information about their microstructure characteristics, as shown in Figure 8. It is clear that the microstructure was strongly affected by the sintering temperature [25,48]. At a magnification of 600  $\mu\text{m}$ , the S650 and S700 membranes exhibited homogeneous surfaces without any macrodefects. At a magnification of 2  $\mu\text{m}$ , SEM images revealed more complex details of the membrane structure. A notable observation was the reduction in the volume of porosity, indicating a reduction in the total volume of the empty space within the membrane. However, the pore size increased, indicating larger openings and channels within the membrane structures. These results suggest that high sintering temperature treatment at 700  $^{\circ}\text{C}$  produced dense membranes with larger pores than at 650  $^{\circ}\text{C}$  and consequently increased membrane permeability (Table 2). Similar findings have been reported in the literature regarding the use of several types of clay for the production of inorganic membranes, demonstrating a correlation between sintering temperature and membrane characteristics, such as a reduction in the porosity volume and an increase in the pore size [25,44,49]. From a higher magnification of 200 nm, it is very clear that the structure of sepiolite membranes involved disordered fibrous layers. The pore sizes of the S650 and S700 membranes, estimated from the SEM results, were around 40 nm and 150 nm, respectively. Therefore, these two membranes work in the domain of ultrafiltration.

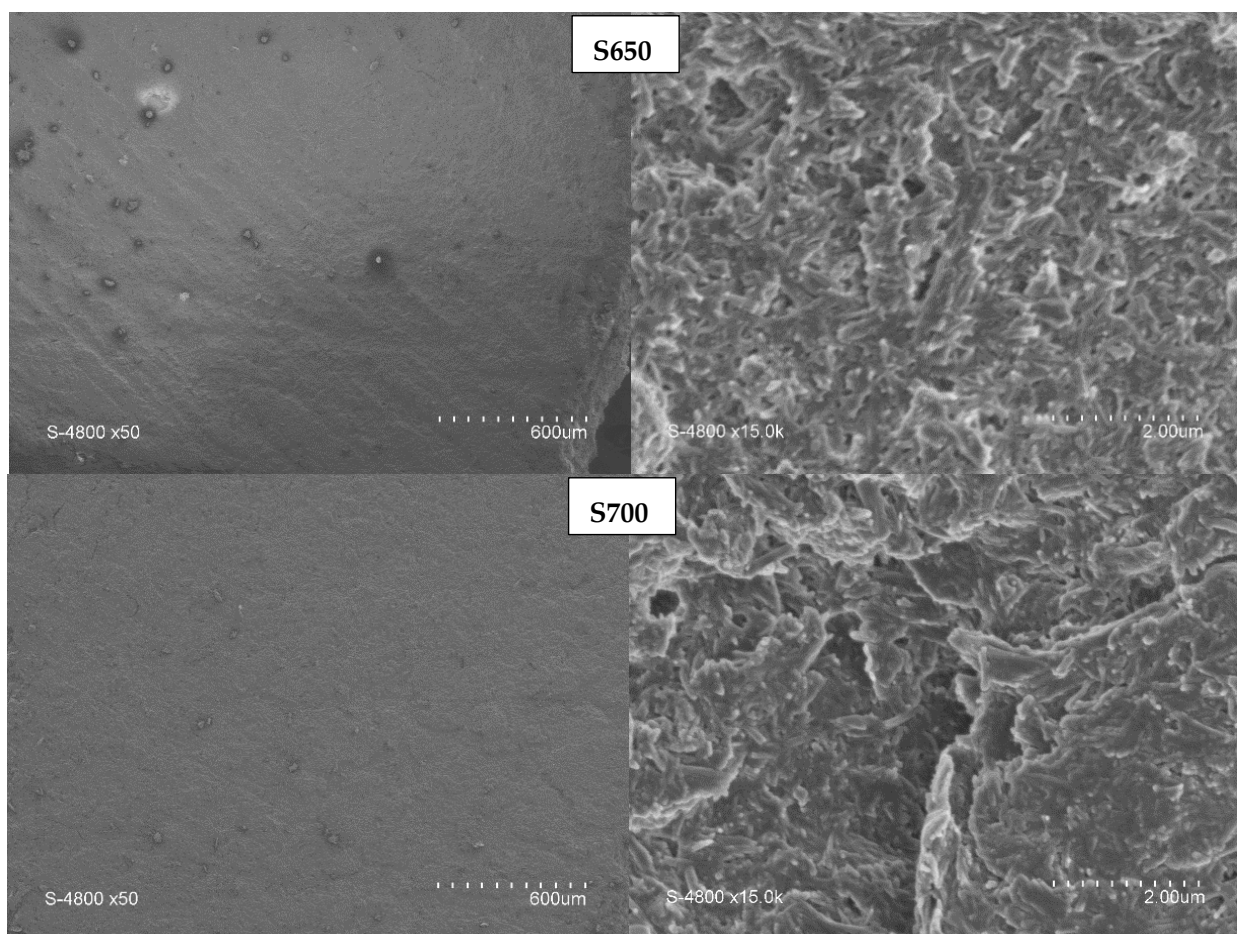


Figure 8. Cont.

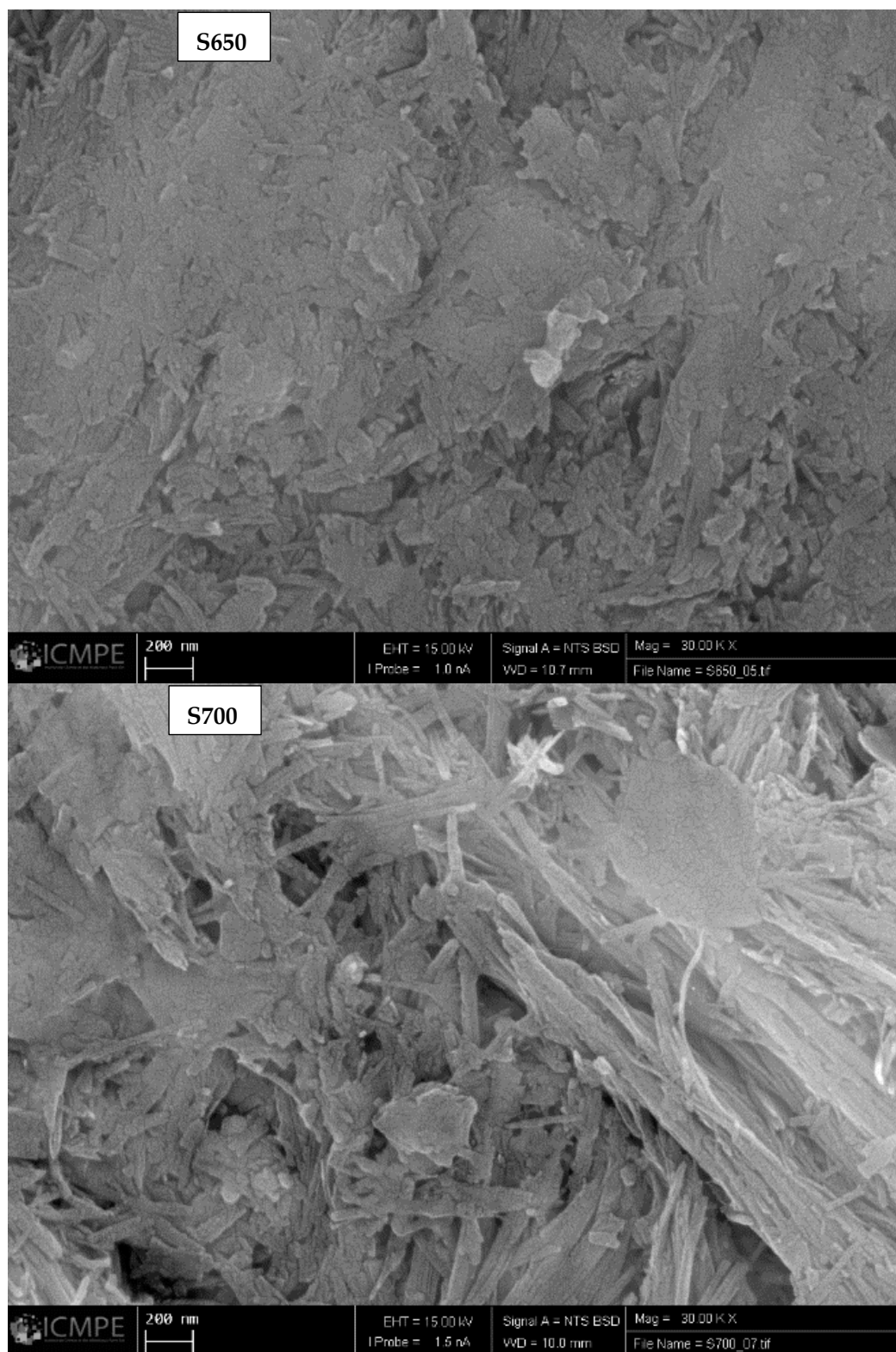


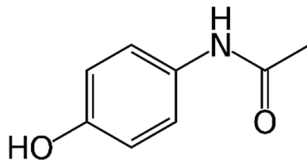
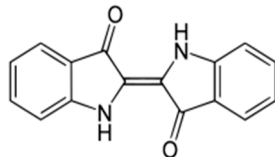
Figure 8. SEM micrographs of S650 and S700 membranes (3 magnifications: 600  $\mu\text{m}$ , 2  $\mu\text{m}$ , and 200 nm).

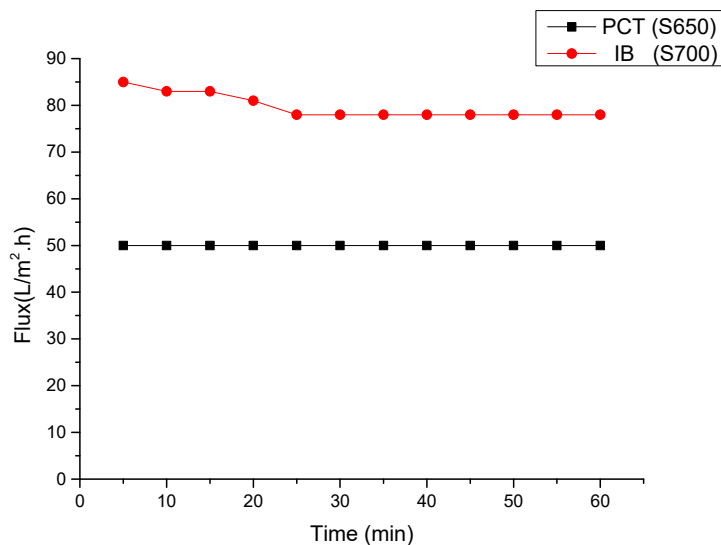
### 3.2.6. Application to Wastewater Treatment

The flat sepiolite membranes S650 and S700 were applied to the treatment of two different synthetic solutions: a paracetamol drug (PCT) aqueous solution and an indigo blue (IB) aqueous solution to assess the efficiency of the membranes for contaminant removal (Table 3). Taking into account the size of the substances to be removed, the S650 membrane

was employed for PCT removal from the PCT solution and the S700 membrane for IB removal from the IB dye solution. Filtration was performed at a transmembrane pressure (TMP) of 3 bar for 60 min. Figure 9 illustrates the evolution of the permeate flux for PCT and IB solution with time. The S650 membrane exhibited a stabilized permeate flux of 50 L/h·m<sup>2</sup> during one hour of filtration for PCT solution. However, for the IB solution treatment using the S700 membrane, the permeate flux decreased slightly from 85 to 78 L/h·m<sup>2</sup> during the first 20 min and then stabilized. The decrease in permeate flux with time is a typical behavior of membranes, which can be explained by the concentration polarization effect and the consequent fouling phenomenon [50]. Thus, the filtration results reveal a good resistance of both membranes to fouling mostly for the couple PCT solution S650.

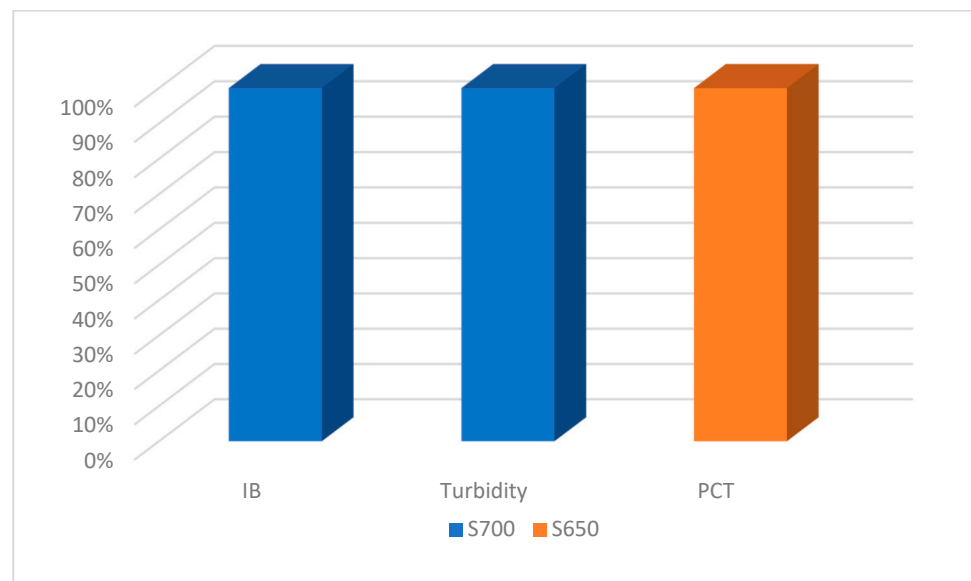
**Table 3.** Characteristics of the synthetic solutions used in this study.

Synthetic Solutions	Chemical Formula	Molecular Weight (g/mol)	Concentration (mg/L)	Turbidity (NTU)	Water Solubility at 25 °C (g/L)	Structural Formula
Paracetamol (PCT)	C <sub>8</sub> H <sub>9</sub> NO <sub>2</sub>	151.16	40	--	2.5	
Indigo Blue (IB)	C <sub>16</sub> H <sub>10</sub> N <sub>2</sub> O <sub>2</sub>	262.26	25	107	--	



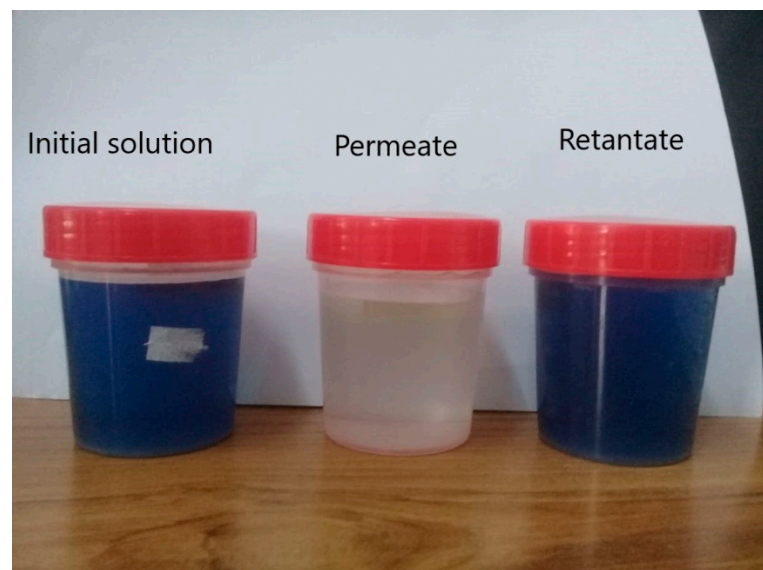
**Figure 9.** Permeate flux versus time during ultrafiltration of PCT and IB solutions by S650 and S700 membranes, respectively (T = 25 °C; TMP = 3 bar; pH of PCT solution = 7.5; pH of IB solution = 11).

Figure 10 shows the complete removal of PCT and IB dye during ultrafiltration. The high PCT retention can be explained by the adsorption of the molecules on the functional groups of the S650 surface [51]. However, the IB retention can be explained by the electrostatic interactions. In fact, according to the pH of the IB solutions, 11, the S700 membrane surface was negatively charged which led to electrostatic repulsion and, consequently, high retention [39].



**Figure 10.** Evolution of the retention percentage of the different pollutants using S650 and S700 membranes.

Figure 11 illustrates the photos of the IB solution before and after ultrafiltration. Total decolorization was observed for the permeate, confirming the high color retention by the S700 membrane. In addition, the permeate seems very clear with high turbidity removal.



**Figure 11.** Photo of IB dye solution before and after treatment with the S700 membrane.

### 3.2.7. Determination of Fouling Coefficients and Membranes Regeneration

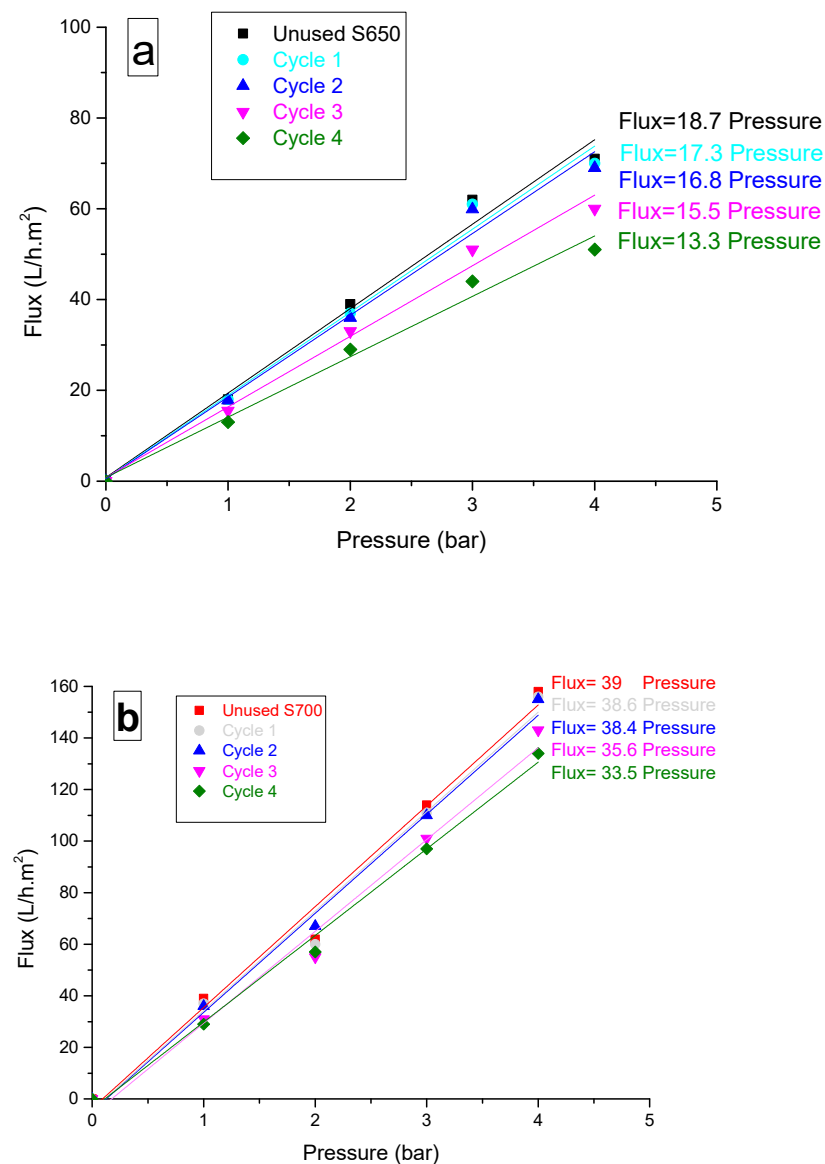
The fouling resistance ability is essential for understanding the efficiency of the membrane. In addition, it has great significance in various filtration applications. It can be evaluated by determining the FRR and FDR coefficients.

Table 4 shows that both S650 and S700 membranes exhibited very high FRR fouling coefficients of 96.7% and 93%, respectively, during the filtration operation of PCT and IB dye aqueous solutions, which confirm the high recovery of permeate flux after regeneration by simple rinsing. This behavior was confirmed by the low FDR values of 18% for S650 and 34% for S700, indicating the slight reduction in permeate flux and, consequently, the lower susceptibility to fouling [36,37]. This finding demonstrates the high anti-fouling

ability of S650 and S700 membranes and their capacity to regain their initial performances after filtration tests. This behavior was not always observed with commercial ceramic membranes or low-cost ceramic membranes fabricated from other starting materials, which require the use of acidic and basic solutions to remove the accumulate foulants and to recover the initial flux after filtration. This operation leads to an increase in the cost of the filtration process taking into account the cost of the various chemicals used and also the decrease in membrane life [14,27]. In this study, membrane regeneration requires only rinsing with deionized water. As shown in Figure 12a,b, the permeability values of the unused and regenerated S650 and S700 membranes were close after four cycles, confirming the efficiency of the cleaning process.

**Table 4.** Determination of the fouling coefficients for S650 and S700 membranes.

Membranes	FRR (%)	FDR (%)
S650	96.7	18
S700	93	34.4



**Figure 12.** Membrane regeneration results after four rinsing cycles for (a) S650 and (b) S700.



#### 4. Conclusions

In this study, low-cost flat ceramic membranes with exclusively sepiolite clay as the raw material were successfully fabricated using an easy method without any organic additives. The determination of the sintering temperature shows that at 650 °C and 750 °C, SEM images exhibit homogeneous structures with average pore diameters of 40 nm (650 °C) and 150 nm (700 °C), mechanical strengths of 18 MPa (650 °C) and 21 MPa (700 °C), and water permeability of 18 L/h·m<sup>2</sup>·bar (650 °C) and 39 L/h·m<sup>2</sup>·bar (700 °C). This finding demonstrates the positive impact of sepiolite material on the membrane preparation conditions. Indeed, a sintering temperature between 1400 and 1600 °C is usually required for commercial ceramic membranes and between 950 and 1150 °C for low-cost ceramic membranes. Comparing sintering temperature as a key indicator of energy consumption during membrane manufacturing indicates that the use of natural zeolite material had a notable impact on reducing the required sintering temperature and, therefore, energy consumption.

Taking into account the average pore size and water permeability, it seems that the manufactured membranes are suitable for UF application.

Subsequently, both membranes were successfully used to eliminate paracetamol drug (PCT) and indigo blue dye (IB) from aqueous solutions. The complete removal of both substances was achieved at an ambient temperature and a pressure of 3 bar.

Moreover, after the filtration process, the sepiolite membranes almost completely recovered their initial performances after simple rinsing with deionized water, which can have a positive effect on the membranes' life duration.

Therefore, this study highlights the importance of choosing a natural and low-cost starting material based on clay for low-cost ceramic membrane fabrication. This choice leads to easy and simple membrane preparation with relatively low sintering temperatures, thus reducing energy consumption and membrane fabrication costs.

**Author Contributions:** Conceptualization, C.C. and R.B.A.; Data curation, M.R.; Investigation, M.R., W.A., C.C., H.A., J.D. and R.B.A.; Methodology, M.R.; Project administration, R.B.A.; Software, M.R., W.A., H.A. and J.D.; Supervision, C.C. and R.B.A.; Validation, C.C., J.D. and R.B.A.; Writing—original draft, M.R., W.A. and H.A.; Writing—review and editing, C.C., J.D. and R.B.A. All authors have read and agreed to the published version of the manuscript.

**Funding:** This study was supported by the PRIMA 2020 program under agreement No\_2024-TRUST project (The PRIMA program is supported by the European Union) and PHC-Utique project 20G1205.

**Institutional Review Board Statement:** Not applicable.

**Informed Consent Statement:** Not applicable.

**Data Availability Statement:** The data presented in this study are available on request from the corresponding author.

**Acknowledgments:** The authors gratefully acknowledge funding from TRUST Prima program (research project supported by the European commission).

**Conflicts of Interest:** The authors declare no conflicts of interest.

#### References

1. Castree, N. Global environmental assessment. *Int. Encycl. Geogr. People Earth Environ. Technol.* **2016**, 1–13. [CrossRef]
2. Mikulic, M. Global Pharmaceutical Industry—Statistics & Facts. Statista. Available online: <https://www.statista.com/topics/1764/global-pharmaceutical-industry> (accessed on 30 August 2019).
3. Kishor, R.; Purchase, D.; Saratale, G.D.; Saratale, R.G.; Ferreira, L.F.R.; Bilal, M.; Chandra, R.; Bharagava, R.N. Ecotoxicological and health concerns of persistent coloring pollutants of textile industry wastewater and treatment approaches for environmental safety. *J. Environ. Chem. Eng.* **2021**, *9*, 105012. [CrossRef]
4. Felis, E.; Kalka, J.; Sochacki, A.; Kowalska, K.; Bajkacz, S.; Harnisz, M.; Korzeniewska, E. Antimicrobial pharmaceuticals in the aquatic environment—occurrence and environmental implications. *Eur. J. Pharmacol.* **2020**, *866*, 172813. [CrossRef]
5. Duan, Z.; Li, Y.; Zhang, M.; Bian, H.; Wang, Y.; Zhu, L.; Xia, D. Towards cleaner wastewater treatment for special removal of cationic organic dye pollutants: A case study on application of supramolecular inclusion technology with  $\beta$ -cyclodextrin derivatives. *J. Clean. Prod.* **2020**, *256*, 120308. [CrossRef]

6. Solayman, H.M.; Hossen, M.A.; Abd Aziz, A.; Yahya, N.Y.; Hon, L.K.; Ching, S.L.; Zoh, K.D. Performance evaluation of dye wastewater treatment technologies: A review. *J. Environ. Chem. Eng.* **2023**, *11*, 109610. [[CrossRef](#)]
7. Almeida, D.L.; Pavanello, A.; Saavedra, L.P.; Pereira, T.S.; de Castro-Prado, M.A.A.; de Freitas Mathias, P.C. Environmental monitoring and the developmental origins of health and disease. *J. Dev. Orig. Health Dis.* **2019**, *10*, 608–615. [[CrossRef](#)]
8. Godoy, A.A.; Kummrow, F. What do we know about the ecotoxicology of pharmaceutical and personal care product mixtures? A critical review. *Crit. Rev. Environ. Sci. Technol.* **2017**, *47*, 1453–1496. [[CrossRef](#)]
9. Peña-Guzmán, C.; Ulloa-Sánchez, S.; Mora, K.; Helena-Bustos, R.; Lopez-Barrera, E.; Alvarez, J.; Rodriguez-Pinzón, M. Emerging pollutants in the urban water cycle in Latin America: A review of the current literature. *J. Environ. Manag.* **2019**, *237*, 408–423. [[CrossRef](#)] [[PubMed](#)]
10. Mittal, J. Permissible synthetic food dyes in India. *Resonance* **2020**, *25*, 567–577. [[CrossRef](#)]
11. Chauhan, B.; Dodamani, S.; Malik, S.; Almalki, W.H.; Haque, S.; Sayyed, R.Z. Microbial approaches for pharmaceutical wastewater recycling and management for sustainable development: A multicomponent approach. *Environ. Res.* **2023**, *237*, 11698. [[CrossRef](#)] [[PubMed](#)]
12. Khan, M.D.; Singh, A.; Khan, M.Z.; Tabraiz, S.; Sheikh, J. Current perspectives, recent advancements, and efficiencies of various dye-containing wastewater treatment technologies. *J. Water Process Eng.* **2023**, *53*, 103579. [[CrossRef](#)]
13. Xu, X.; Shao, W.; Tai, G.; Yu, M.; Han, X.; Han, J.; Xing, W. Single-atomic Co-N site modulated exciton dissociation and charge transfer on covalent organic frameworks for efficient antibiotics degradation via peroxymonosulfate activation. *Sep. Purif. Technol.* **2024**, *333*, 125890. [[CrossRef](#)]
14. Mouiya, M.; Abourriche, A.; Bouazizi, A.; Benhammou, A.; El Hafiane, Y.; Abouliatim, Y.; Nibou, L.; Oumam, M.; Ouammou, M.; Smith, A.; et al. Flat ceramic microfiltration membrane based on natural clay and Moroccan phosphate for desalination and industrial wastewater treatment. *Desalination* **2018**, *427*, 42–50. [[CrossRef](#)]
15. Rani, S.L.S.; Kumar, R.V. Insights on applications of low-cost ceramic membranes in wastewater treatment: A mini-review. *Case Stud. Chem. Environ. Eng.* **2021**, *4*, 100149. [[CrossRef](#)]
16. Kujawska, A.; Kielkowska, U.; Atisha, A.; Yanful, E.; Kujawski, W. Comparative analysis of separation methods used for the elimination of pharmaceuticals and personal care products (PPCPs) from water—A critical review. *Sep. Purif. Technol.* **2022**, *290*, 120797. [[CrossRef](#)]
17. Yeom, H.J.; Kim, S.C.; Kim, Y.W.; Song, I.H. Processing of alumina-coated clay–diatomite composite membranes for oily wastewater treatment. *Ceram. Int.* **2016**, *42*, 5024–5035. [[CrossRef](#)]
18. Issaoui, M.; Limousy, L. Low-cost ceramic membranes: Synthesis, classifications, and applications. *Comptes Rendus Chim.* **2019**, *22*, 175–187. [[CrossRef](#)]
19. Oatley-Radcliffe, D.L.; Walters, M.; Ainscough, T.J.; Williams, P.M.; Mohammad, A.W.; Hilal, N. Nanofiltration membranes and processes: A review of research trends over the past decade. *J. Water Process Eng.* **2017**, *19*, 164–171. [[CrossRef](#)]
20. Cao, D.Q.; Yang, X.X.; Yang, W.Y.; Wang, Q.H.; Hao, X.D. Separation of trace pharmaceuticals individually and in combination via forward osmosis. *Sci. Total Environ.* **2020**, *718*, 137366. [[CrossRef](#)] [[PubMed](#)]
21. Van der Bruggen, B.; Mänttari, M.; Nyström, M. Drawbacks of applying nanofiltration and how to avoid them: A review. *Sep. Purif. Technol.* **2008**, *63*, 251–263. [[CrossRef](#)]
22. Abdullayev, A.; Bekheet, M.F.; Hanaor, D.A.; Gurlo, A. Materials and applications for low-cost ceramic membranes. *Membranes* **2019**, *9*, 105. [[CrossRef](#)]
23. Dilaver, M.; Hocaoglu, S.M.; Soydemir, G.; Dursun, M.; Keskinler, B.; Koyuncu, İ.; Ağtaş, M. Hot wastewater recovery by using ceramic membrane ultrafiltration and its reusability in textile industry. *J. Clean. Prod.* **2018**, *171*, 220–233. [[CrossRef](#)]
24. Talidia, A.; Bouazizib, A.; Essated, A.; Karimd, A.; Aaddaned, A.; Ouammou, M.; Younssi, S.A. Manufacture and characterization of flat microfiltration membrane based on Moroccan pyrophyllite clay for pretreatment of raw seawater for desalination. *Desalination Water Treat.* **2022**, *253*, 24–38. [[CrossRef](#)]
25. Saja, S.; Bouazizi, A.; Achiou, B.; Ouammou, M.; Albizane, A.; Bennazha, J.; Younssi, S.A. Elaboration and characterization of low-cost ceramic membrane made from natural Moroccan perlite for treatment of industrial wastewater. *J. Environ. Chem. Eng.* **2018**, *6*, 451–458. [[CrossRef](#)]
26. Kim, S.; Park, C. Fouling behavior and cleaning strategies of ceramic ultrafiltration membranes for the treatment and reuse of laundry wastewater. *J. Water Process Eng.* **2022**, *48*, 102840. [[CrossRef](#)]
27. Kumar, R.V.; Ghoshal, A.K.; Pugazhenthii, G. Elaboration of novel tubular ceramic membrane from inexpensive raw materials by extrusion method and its performance in microfiltration of synthetic oily wastewater treatment. *J. Membr. Sci.* **2015**, *490*, 92–102. [[CrossRef](#)]
28. Bouazizi, A.; Saja, S.; Achiou, B.; Ouammou, M.; Calvo, J.I.; Aaddane, A.; Younssi, S.A. Elaboration and characterization of a new flat ceramic MF membrane made from natural Moroccan bentonite. Application to treatment of industrial wastewater. *Appl. Clay Sci.* **2016**, *132*, 33–40. [[CrossRef](#)]
29. Bouazizi, A.; Breida, M.; Achiou, B.; Ouammou, M.; Calvo, J.I.; Aaddane, A.; Younssi, S.A. Removal of dyes by a new nano-TiO<sub>2</sub> ultrafiltration membrane deposited on low-cost support prepared from natural Moroccan bentonite. *Appl. Clay Sci.* **2017**, *149*, 127–135. [[CrossRef](#)]

30. Bousbih, S.; Errais, E.; Darragi, F.; Duplay, J.; Trabelsi-Ayadi, M.; Daramola, M.O.; Ben Amar, R. Treatment of textile wastewater using monolayered ultrafiltration ceramic membrane fabricated from natural kaolin clay. *Environ. Technol.* **2021**, *42*, 3348–3359. [[CrossRef](#)]
31. Wang, Q.K.; Matsuura, T.; Feng, C.Y.; Weir, M.R.; Detellier, C.; Rutadinka, E.; Van Mao, R.L. The sepiolite membrane for ultrafiltration. *J. Membr. Sci.* **2001**, *184*, 153–163. [[CrossRef](#)]
32. Masood, F.; ul Ain, N.; Habib, S.; Alam, A.; Yasin, T.; Hameed, A.; Farooq, M. Preparation, characterization, and evaluation of multifunctional properties of PVA/metal oxide@ sepiolite nanocomposite membranes for water cleanup. *Mater. Today Commun.* **2022**, *31*, 103620. [[CrossRef](#)]
33. Tian, G.; Han, G.; Wang, F.; Liang, J. Sepiolite nanomaterials: Structure, properties and functional applications. In *Nanomaterials from Clay Minerals*; Elsevier: Amsterdam, The Netherlands, 2019; pp. 135–201.
34. Post, J.E.; Bish, D.L.; Heaney, P.J. Synchrotron powder X-ray diffraction study of the structure and dehydration behavior of sepiolite. *Am. Miner.* **2007**, *92*, 91–97. [[CrossRef](#)]
35. Liu, W.; Canfield, N. Development of thin porous metal sheet as micro-filtration membrane and inorganic membrane support. *J. Membr. Sci.* **2012**, *409*, 113–126. [[CrossRef](#)]
36. Romdhani, M.; Aloulou, W.; Aloulou, H.; Charcosset, C.; Mahouche-Chergui, S.; Carbonnier, B.; Amar, R.B. Performance studies of indigo dye removal using TiO<sub>2</sub> modified clay and zeolite ultrafiltration membrane hybrid system. *Desalination Water Treat.* **2021**, *243*, 262–274. [[CrossRef](#)]
37. Veréb, G.; Kassai, P.; Nascimben Santos, E.; Arthanareeswaran, G.; Hodúr, C.; László, Z. Intensification of the ultrafiltration of real oil-contaminated (produced) water with pre-ozonation and/or with TiO<sub>2</sub>, TiO<sub>2</sub>/CNT nanomaterial-coated membrane surfaces. *Environ. Sci. Pollut. Res.* **2020**, *27*, 22195–22205. [[CrossRef](#)] [[PubMed](#)]
38. Aloulou, H.; Aloulou, W.; Duplay, J.; Baklouti, L.; Dammak, L.; Ben Amar, R. Development of Ultrafiltration Kaolin Membranes over Sand and Zeolite Supports for the Treatment of Electroplating Wastewater. *Membranes* **2022**, *12*, 1066. [[CrossRef](#)] [[PubMed](#)]
39. Largo, F.; Haounati, R.; Akhouairi, S.; Ouachtak, H.; El Haouti, R.; El Guerdaoui, A.; Hafid, N.; Santos, D.M.; Akbal, F.; Kuleyin, A.; et al. Adsorptive removal of both cationic and anionic dyes by using sepiolite clay mineral as adsorbent: Experimental and molecular dynamic simulation studies. *J. Mol. Liq.* **2020**, *318*, 114247. [[CrossRef](#)]
40. Papoulis, D.; Panagiotaras, D.; Tsigrou, P.; Christoforidis, K.C.; Petit, C.; Apostolopoulou, A.; Stathatos, E.; Komarneni, S.; Koukouvelas, I. Halloysite and sepiolite–TiO<sub>2</sub> nanocomposites: Synthesis characterization and photocatalytic activity in three aquatic wastes. *Mater. Sci. Semicond. Process.* **2018**, *85*, 1–8. [[CrossRef](#)]
41. Tabak, A.; Eren, E.; Afsin, B.; Caglar, B.Ü.L.E.N.T. Determination of adsorptive properties of a Turkish Sepiolite for removal of Reactive Blue 15 anionic dye from aqueous solutions. *J. Hazard. Mater.* **2009**, *161*, 1087–1094. [[CrossRef](#)]
42. Frost, R.; Kristóf, J.; Horváth, E. Controlled rate thermal analysis of sepiolite. *J. Therm. Anal. Calorim.* **2009**, *98*, 423–428. [[CrossRef](#)]
43. Zhang, Y.; Wang, L.; Wang, F.; Liang, J.; Ran, S.; Sun, J. Phase transformation and morphology evolution of sepiolite fibers during thermal treatment. *Appl. Clay Sci.* **2017**, *143*, 205–211. [[CrossRef](#)]
44. Sahnoun, R.D.; Baklouti, S. Characterization of flat ceramic membrane supports prepared with kaolin-phosphoric acid-starch. *Appl. Clay Sci.* **2013**, *83*, 399–404. [[CrossRef](#)]
45. Sayehi, M.; Sahnoun, R.D.; Fakhfakh, S.; Baklouti, S. Effect of elaboration parameters of a membrane ceramic on the filtration process efficacy. *Ceram. Int.* **2018**, *44*, 5202–5208. [[CrossRef](#)]
46. Chihi, R.; Blidi, I.; Trabelsi-Ayadi, M.; Ayari, F. Elaboration and characterization of a low-cost porous ceramic support from natural Tunisian bentonite clay. *Comptes Rendus Chim.* **2019**, *22*, 188–197. [[CrossRef](#)]
47. Hamid, Y.; Tang, L.; Hussain, B.; Usman, M.; Liu, L.; Ulhassan, Z.; He, Z.; Yang, X. Sepiolite clay: A review of its applications to immobilize toxic metals in contaminated soils and its implications in soil–plant system. *Environ. Technol. Innov.* **2021**, *23*, 101598. [[CrossRef](#)]
48. Elomari, H.; Achiou, B.; Ouammou, M.; Albizane, A.; Bennazha, J.; Alami Younssi, S.; Elamrani, I. Elaboration and characterization of flat membrane supports from Moroccan clays. Application for the treatment of wastewater. *Desalination Water Treat.* **2016**, *57*, 20298–20306. [[CrossRef](#)]
49. Fakhfakh, S.; Baklouti, S.; Bouaziz, J. Elaboration and characterisation of low cost ceramic support membrane. *Adv. Appl. Ceram.* **2010**, *109*, 31–38. [[CrossRef](#)]
50. Field, R.W.; Wu, J.J. On boundary layers and the attenuation of driving forces in forward osmosis and other membrane processes. *Desalination* **2018**, *429*, 167–174. [[CrossRef](#)]
51. Matin, A.; Jillani, S.M.S.; Baig, U.; Ihsanullah, I.; Alhooshani, K. Removal of pharmaceutically active compounds from water sources using nanofiltration and reverse osmosis membranes: Comparison of removal efficiencies and in-depth analysis of rejection mechanisms. *J. Environ. Manag.* **2023**, *338*, 117682. [[CrossRef](#)]

**Disclaimer/Publisher’s Note:** The statements, opinions and data contained in all publications are solely those of the individual author(s) and contributor(s) and not of MDPI and/or the editor(s). MDPI and/or the editor(s) disclaim responsibility for any injury to people or property resulting from any ideas, methods, instructions or products referred to in the content.